Equatorially Trapped Waves in Shallow Water

David Randall

Introduction

Matsuno (1966; Fig. 1) studied the linearized shallow water equations applied to an equatorial β-plane:

$$\begin{aligned} \frac{\partial u}{\partial t} - fv + g\frac{\partial h}{\partial x} &= 0, \\ \frac{\partial v}{\partial t} + fu + g\frac{\partial h}{\partial y} &= 0, \\ \frac{\partial h}{\partial t} + H\left(\frac{\partial u}{\partial x} + \frac{\partial v}{\partial y}\right) &= 0. \end{aligned} \tag{1}$$

Here $f \equiv \beta y$, where y is distance in the meridional direction, measured from $y = 0$ at the Equator (i.e., $y = a\varphi$), and $\beta \equiv \frac{df}{dy}$ is approximated by a constant value.

Figure 1: Prof. T. Matsuno, giving a lecture at UCLA in January 1998.

Matsuno defined a time scale, $T \equiv \sqrt{\frac{1}{c\beta}}$, and a length scale, $L \equiv \sqrt{\frac{c}{\beta}}$. Here $c \equiv \sqrt{gH}$ is the phase speed of a pure gravity wave. With these length and time scales, the velocity scale is simply c . See Fig. 2 for a sketch defining the other quantities. The length L can be interpreted as the "Equatorial radius of deformation." For $c = 10$ m s^{-1}, we find that $L = 1000$ km and $T \cong 1$ day. Nondimensionalizing the governing equations by T and L , we obtain

Copyright David Randall, 2012

$$\frac{\partial u}{\partial t} - yv + \frac{\partial \phi}{\partial x} = 0,$$
$$\frac{\partial v}{\partial t} + yu + \frac{\partial \phi}{\partial y} = 0,$$
$$\frac{\partial \phi}{\partial t} + \frac{\partial u}{\partial x} + \frac{\partial v}{\partial y} = 0. \tag{2}$$

Here ϕ is the non-dimensional form of gh.

As a side comment, we note that these equations can actually apply to a model with vertical structure (e.g. McCreary, 1981), and so are more readily applicable to the real atmosphere than one might guess. For example, consider a two-level model:

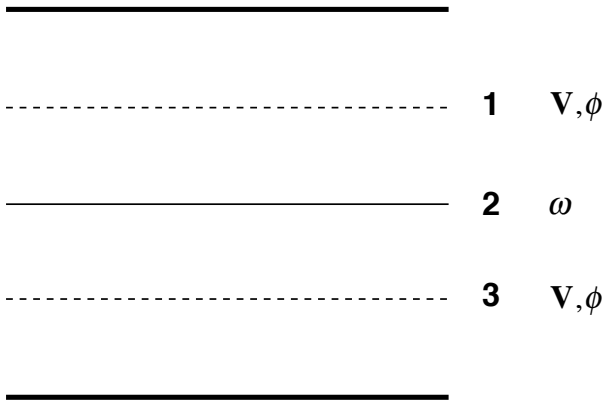

Figure 2: Schematic used to explain the two-level model represented by Eqs. (3).

$$\frac{\partial \mathbf{V}_1}{\partial t} + f\mathbf{k} \times \mathbf{V}_1 + \nabla \phi_1 = 0,$$
$$\frac{\partial \mathbf{V}_3}{\partial t} + f\mathbf{k} \times \mathbf{V}_3 + \nabla \phi_3 = 0,$$
$$\frac{\partial}{\partial t}(\phi_3 - \phi_1) + S\Delta p \omega_2 = 0. \tag{3}$$

As shown in Fig. 2, subscript 1 denotes the upper level and subscript 3 denotes the lower level. The vertical velocity is defined in between, at level 2. Here $\Delta p \equiv p_3 - p_1$ is the pressure thickness between the two layers, and $S \equiv -\frac{\alpha}{\theta}\frac{\partial \theta}{\partial p}$ is the static stability of the basic state. Let

$$\mathbf{V}_d \equiv \mathbf{V}_3 - V_1 , \tag{4}$$

$$\phi_d \equiv \phi_3 - \phi_1 , \tag{5}$$

be the vertical shear (actually, difference) of the horizontal wind between the two layers, and the thickness between the two layers, respectively. Then (3) implies that

$$\frac{\partial \mathbf{V}_d}{\partial t} + f\mathbf{k} \times \mathbf{V}_d + \nabla \phi_d = 0 , \tag{6}$$

and

Copyright David Randall, 2012

$$\frac{\partial \phi_d}{\partial t} + \frac{S\Delta p^2}{2} \nabla \cdot \mathbf{V}_d = 0 \,, \tag{7}$$

which are identical to the shallow water equations, and we can identify

$$c_i \equiv \Delta p \sqrt{\frac{S}{2}} \tag{8}$$

as the phase-speed of the internal gravity waves.

We return now to our discussion of (2). Assume solutions of the form

$$\begin{aligned} u &= \hat{u}(y) e^{i(kx+\omega t)}, \\ v &= \hat{v}(y) e^{i(kx+\omega t)}, \\ \phi &= \hat{\phi}(y) e^{i(kx+\omega t)} \,. \end{aligned} \tag{9}$$

If we adopt the convention that k is positive, then $\omega > 0$ corresponds to westward propagation, and $\omega < 0$ to eastward propagation. Substitution into (2) gives

$$\begin{aligned} i\omega\hat{u} - y\hat{v} + ik\hat{\phi} &= 0, \\ i\omega\hat{v} + y\hat{u} + \frac{d\hat{\phi}}{dy} &= 0, \\ i\omega\hat{\phi} + ik\hat{u} + \frac{d\hat{v}}{dy} &= 0. \end{aligned} \tag{10}$$

The first of these equations can be solved for $\hat{u}$ in terms of $\hat{v}$ and $\hat{\phi}$, and the result can be used to eliminate $\hat{u}$ in the other two equations. Then the system (10) can be rewritten as

$$\begin{aligned} \omega\hat{u} &= -k\hat{\phi} - iy\hat{v}, \\ ky\hat{\phi} - \omega\frac{d\hat{\phi}}{dy} &= i\left(\omega^2 - y^2\right)\hat{v}, \\ \left(\omega^2 - k^2\right)\hat{\phi} &= i\left(ky\hat{v} + \omega\frac{d\hat{v}}{dy} \right). \end{aligned} \tag{11}$$

Kelvin waves

There is a special solution, called the Kelvin wave, for which the meridional wind is identically zero. In that case, (11) reduces to

Copyright David Randall, 2012

$$\begin{aligned} \omega\hat{u} &= -k\hat{\phi}, \\ ky\hat{\phi} - \omega\frac{d\hat{\phi}}{dy} &= 0, \\ \left(\omega^2 - k^2\right)\hat{\phi} &= 0. \end{aligned} \tag{12}$$

The third of these implies that, for non-trivial solutions,

$$\omega = \pm k\ . \tag{13}$$

With the use and inclusion of (13), our system becomes

$$\begin{aligned} \pm\hat{u} &= -\hat{\phi}, \\ -y\hat{\phi} \pm \frac{d\hat{\phi}}{dy} &= 0, \\ \omega &= \pm k \end{aligned} \tag{14}$$

The middle equation obviously determines the meridional structure of ϕ. The solution is

$$\hat{\phi} = e^{\pm y^2/2}\ . \tag{15}$$

Here the plus and minus signs correspond to those used in (13). If we choose the plus sign, we get solutions that grow exponentially away from the Equator, which is unacceptable, especially since the Equatorial beta plane approximation is only useful near the Equator. We therefore choose the minus sign in (14)-(15). In (15), this gives a "bell-shaped" solution with a maximum on the Equator, and symmetry across the Equator. The solution can be written as

$$\begin{aligned} \hat{u} &= e^{-y^2/2}, \\ \hat{\phi} &= e^{-y^2/2}, \\ \omega &= -k. \end{aligned} \tag{16}$$

Note that $\omega = -k$ implies eastward propagation.

Other solutions

Returning now to the general case, we can combine the second and third equations of (11) to obtain

Copyright David Randall, 2012

$$ky\left(ky\hat{v}+\omega\frac{d}{dy}\hat{v}\right)-\omega\frac{d}{dy}\left(ky\hat{v}+\omega\frac{d}{dy}\hat{v}\right)=\left(\omega^2-k^2\right)\left(\omega^2-y^2\right)\hat{v}\,,$$

(17)

which can be simplified to

$$\boxed{\frac{d^2\hat{v}}{dy^2}+\left(\omega^2-k^2+\frac{k}{\omega}-y^2\right)\hat{v}=0}\,.$$

(18)

Note that the substitution used to obtain (17)-(18) is only valid for $\omega^2-k^2\neq 0$. Therefore, (18) does not apply to the Kelvin wave, for which $\omega^2-k^2=0$.

We expect the solutions of (18) to have "wavy" behavior for $\omega^2-k^2+\frac{k}{\omega}-y^2>0$, and exponential behavior for $\omega^2-k^2+\frac{k}{\omega}-y^2<0$. Because of the $-y^2$ term, exponential behavior will emerge sufficiently far from the Equator, and, as with the Kelvin wave, we want this to be exponential decay rather than exponential growth. Therefore, as boundary conditions, we use

$$\hat{v}\to 0 \text{ as } y\to\pm\infty\,.$$

(19)

It can be shown that nontrivial solutions satisfying these boundary conditions exist when

$$\boxed{\omega^2-k^2+\frac{k}{\omega}=2n+1 \text{ for } n=0,\ 1,\ 2\ldots}\,.$$

(20)

Note that the expression on the right-hand side of (20) generates all positive odd integers, so that Eq. (20) is equivalent to the statement that $\omega^2-k^2+\frac{k}{\omega}$ is an odd positive integer.

Notice, however, that (20) will give $\omega=-k$ if we set $n=-1$. For this reason, it is convenient to think of the Kelvin wave as the solution corresponding to $n=-1$, and this will be used in Fig. 3, to be discussed later.

You can verify by substitution that the solutions of (18) are

$$\hat{v}(y)=Ce^{-\frac{1}{2}y^2}H_n(y)\,,$$

(21)

where $H_n(y)$ is the *n*th Hermite polynomial, which is given by

Copyright David Randall, 2012

$$H_n(y) \equiv (-1)^n e^{y^2} \frac{d^n}{dy^n}\left(e^{-y^2}\right).$$

(22)

(See the *QuickStudy* on Hermite polynomials.) As already mentioned, the factor e^{-y^2} ensures that these modes decay rapidly away from the Equator. The *e*-folding distance is about 1000 km.

The dispersion equation, (20), is cubic in ω, and so there are three ωs for each (k,n) pair. Two of these correspond to inertia-gravity waves. For large k, they can be approximated by

$$\omega_{1,2} \cong \pm\sqrt{k^2 + 2n + 1}.$$

(23)

These expressions can be compared with (38). The third root of (20) corresponds to a Rossby wave. For *small* k, it can be approximated by

$$\omega_3 \cong \frac{k}{k^2 + 2n + 1}.$$

(24)

For the special case $n = 0$, the equations simplify quite a bit. First of all, $H_0(y) = 1$ for all y, so the meridional structure of $\hat{v}(y)$, given by (21) is simply the bell-shaped Gaussian curve. This means that the meridional velocity has the same sign on both sides of the Equator and is a maximum on the Equator.

In addition, for $n = 0$ the dispersion equation (20) can be factored:

$$(\omega - k)\left(\omega^2 + k\omega - 1\right) = 0 \text{ for } n = 0.$$

(25)

Matsuno showed that the three roots of (25) can be interpreted as follows:

$$\text{Eastward gravity wave: } \omega_1 = -\frac{k}{2} - \sqrt{\left(\frac{k}{2}\right)^2 + 1} \text{ for } n = 0,$$

(26)

$$\text{Westward gravity wave: } \omega_2 = \begin{cases} -\frac{k}{2} + \sqrt{\left(\frac{k}{2}\right)^2 + 1} & \text{for } k \le \frac{1}{\sqrt{2}} \\ k & \text{for } k \ge \frac{1}{\sqrt{2}} \end{cases} \text{ for } n = 0,$$

(27)

Copyright David Randall, 2012

$$\text{Rossby wave: } \omega_3 = \begin{cases} k & \text{for } k \le \dfrac{1}{\sqrt{2}} \\ -\dfrac{k}{2} + \sqrt{\left(\dfrac{k}{2}\right)^2 + 1} & \text{for } k \ge \dfrac{1}{\sqrt{2}} \end{cases} \quad \text{for } n = 0 \,. \tag{28}$$

The westward gravity wave described by (27) and the Rossby wave described by (28) are not really distinct. They coincide for $k = 1/\sqrt{2}$. For reasons discussed just below Eq. (18), the root $\omega = k$ has to be thrown out. Matsuno concluded, therefore, that for $n = 0$ we really have only two waves: an eastward moving gravity wave, and a "mixed Rossby-gravity wave," which is also called the "Yanai wave," after the late Prof. Michio Yanai[1] of UCLA. The Yanai wave behaves like a gravity wave for $k < 1/\sqrt{2}$, and like a Rossby wave for $k > 1/\sqrt{2}$. The dispersion relation for the Yanai wave is

Figure 1: Prof. Michio Yanai.

$$\omega = \sqrt{\left(\frac{k}{2}\right)^2 + 1} - \frac{k}{2} \,. \tag{29}$$

Substituting $k = 1/\sqrt{2}$ in (29) gives $\omega = 1/\sqrt{2}$, so that $\omega = k$.

The various wave-solutions of Matsuno's model are summarized in Fig. 3, which shows the roots of the dispersion equation. Recall that positive values of the frequency correspond to westward propagating waves, and negative values (lower part of the figure) to eastward propagating waves. The thick solid curves arcing upward from the origin represent Rossby waves, with positive values of . The dashed curves in the upper part of the diagram correspond to westward propagating inertia-gravity waves, and the thin solid curves in the lower part of the diagram correspond to eastward propagating inertia gravity waves.

The westward propagating wave represented by the curve that is partly solid and partly dashed is the mixed Rossby-gravity wave, or Yanai wave. The dashed portion of this curve, plotted for $k < 1/\sqrt{2}$, represents those wave numbers for which the Yanai wave behaves like a westward propagating gravity wave. The solid portion of the curve, for $k > 1/\sqrt{2}$, represents those wave numbers for which the Yanai wave behaves like a Rossby wave.

---

[1] Yanai and Matsuno shared an office in graduate school.

Copyright David Randall, 2012

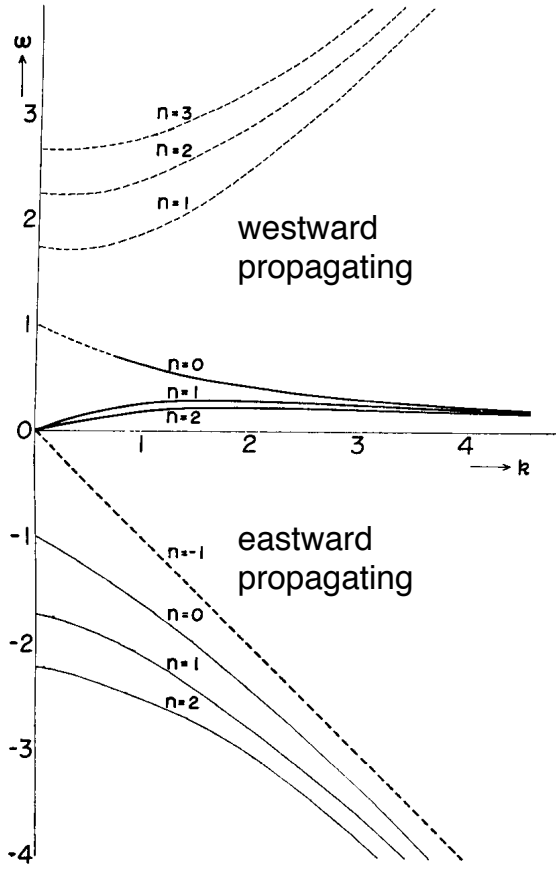

Figure 3: Frequencies as functions of wave number. Positive frequencies correspond to westward propagation. Thin solid line: eastward propagating inertia-gravity waves. Thin dashed line: westward propagating inertia-gravity waves. Thick solid line: Rossby (quasi-geostrophic) waves. Thick dashed line: The Kelvin wave. The westward moving wave with $n = 0$ is the Yanai wave. It is denoted by a dashed line for $k < 1/\sqrt{2}$, and by a solid line for $k > 1/\sqrt{2}$. From Matsuno (1966).

The dashed line proceeding down and towards the right from the origin represents the Kelvin wave.

For $n = 0$, the eastward moving inertia-gravity wave and westward moving Yanai wave have the structures shown in the upper and middle panels of Fig. 4. For a pure gravity wave we expect the winds to be perpendicular to the isobars. When rotation is dominant, the winds are parallel to the isobars. The waves shown look like pure gravity waves near the Equator. For $n = 0$ and $k = 1$, the Yanai wave takes on the characteristics of a Rossby wave, as shown in the lower panel.

Copyright David Randall, 2012

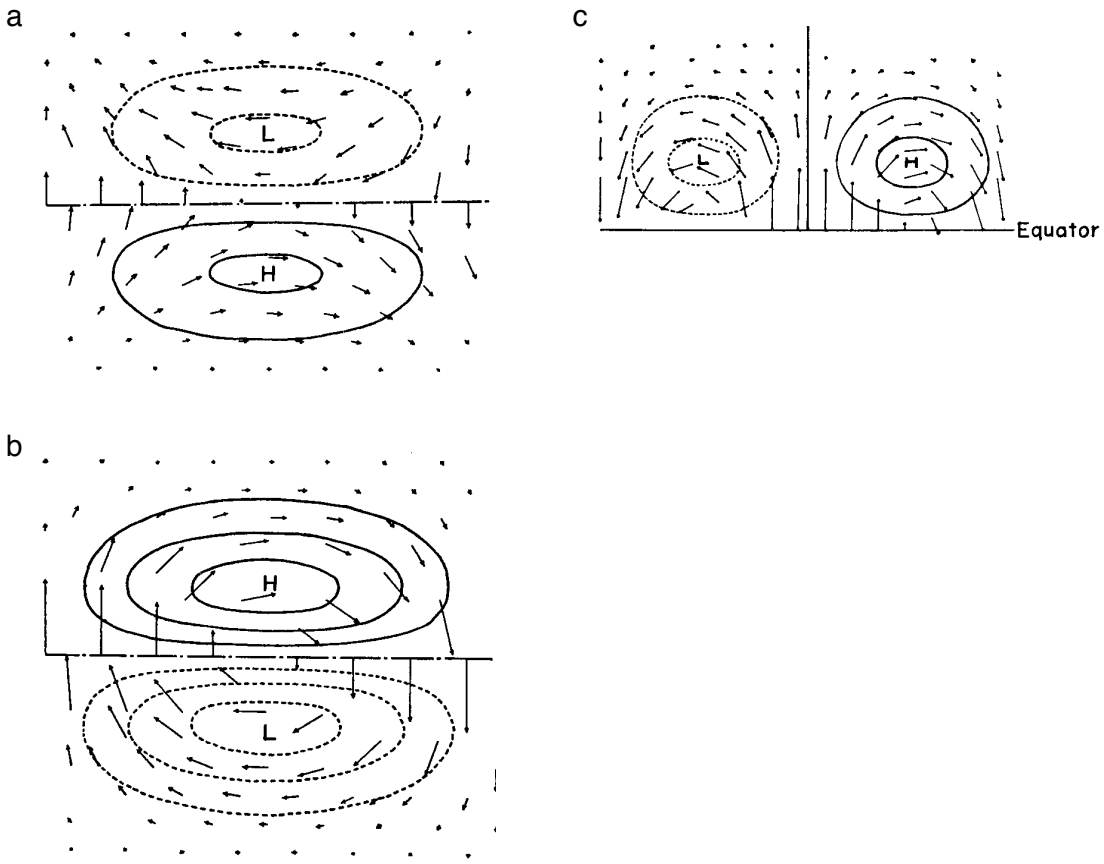

Figure 4: Pressure and velocity distributions of solutions for $n = 0$ and $k = 0.5$. a) Eastward moving inertia-gravity wave. b) Westward moving Yanai wave, which for this value of k behaves like an inertia-gravity wave. c) The structure of the Yanai wave for $n = 0$ and $k = 1$, in which case the Yanai wave acts like a Rossby wave. For each mode, v is a maximum on the Equator and does not pass through zero anywhere. This is characteristic of $n = 0$. From Matsuno (1966).

Solutions for $n = 1$ are shown on the left side of Fig. 5. The corresponding results for $n = 2$ are shown on the right side of the figure. Recall that the subscript n denotes the solution whose meridional structure is described by the n th Hermite polynomial. As can be seen in the figure, higher values of correspond to more nodes in the meridional direction.

Copyright David Randall, 2012

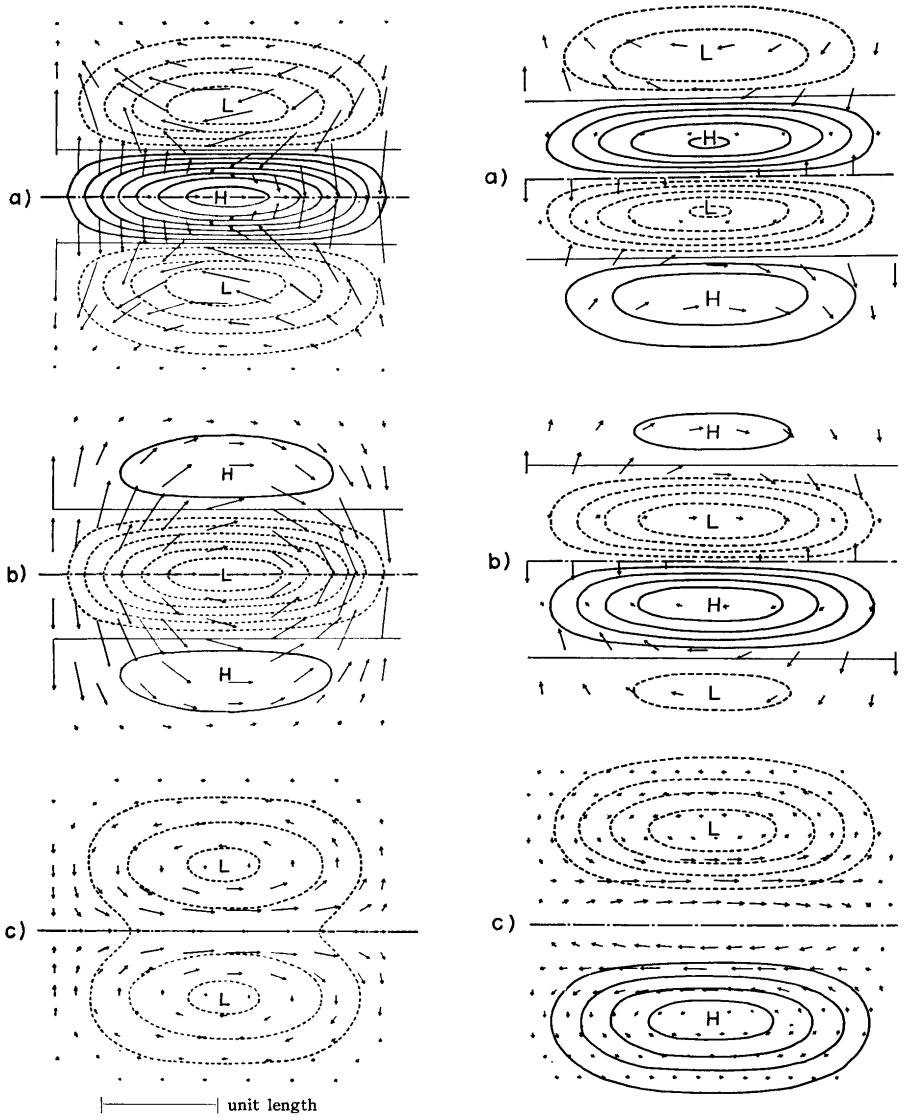

Figure 5: Left side: Pressure and velocity distributions of solutions for $n=1$. a) Eastward propagating inertia-gravity wave. For each mode, $u=0$ on the Equator, as we expect for $n=1$. b) Westward propagating inertia-gravity wave. c) Rossby wave. Right side: Corresponding results for $n=2$. For each mode, u is symmetrical across the Equation, as we expect for $n=2$. From Matsuno (1966).

The structure of the Kelvin wave is shown in Fig. 6. Note that the velocity vectors are purely zonal, and that the tendency of the zonal wind is in phase with the pressure, as in a gravity wave.

Copyright David Randall, 2012

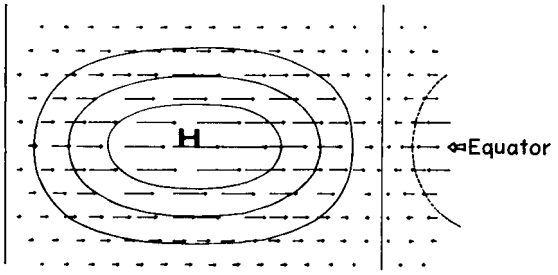

Figure 6: Pressure and velocity distributions for $n=-1$ and $k=0.5$. This is a Kelvin wave. From Matsuno (1966).

There have been many observational studies of tropical waves. Yanai and Maruyama (1966) and Maruyama and Yanai (1967) observed the mixed-Rossby-gravity wave shortly after Matsuno had predicted its existence. Wallace and Kousky (1968) found the Kelvin wave shortly thereafter. This is a spectacular example of theoretical work (Matsuno, 1966) foreshadowing observational discoveries.

In more modern work, Wheeler and Kiladis (1999) examined the space-time variability of the tropical outgoing long wave radiation.In Fig. 7, the data have been separated into modes that are symmetric across the Equator (right panel), such as the Kelvin wave, and modes that are anti-symmetric across the Equator (left panel), such as the mixed-Rossby-gravity wave. Through the use of additional filtering procedures motivated by Matsuno's results, Wheeler and Kiladis were able to show the longitudinal propagation of various types of equatorially trapped disturbances, as shown in Figs. 7-8.

The response of the tropical atmosphere to stationary heat sources and sinks

The discussion above is all about "free waves." Forced solutions to Matsuno's model are also of great importance. Fig. 9, which is taken from Matsuno (1966), shows the stationary

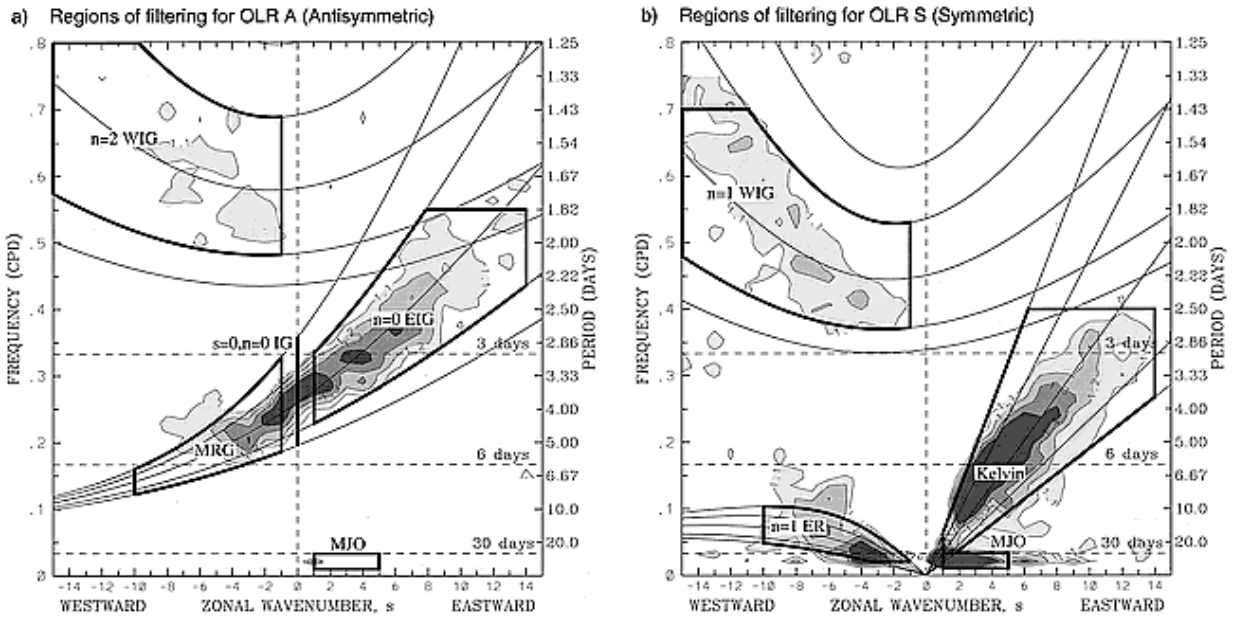

Figure 7: The variability of the outgoing longwave radiation (OLR) as a function of frequency and zonal wave number for modes that are symmetric across the Equator (right panel) and anti-symmetric (left panel). Eastward propagation is associated with positive wave numbers, and vice versa. The boxes select particular wave types. From Wheeler and Kiladis (1999).

Copyright David Randall, 2012

circulation driven by a mass source and sink on the Equator. Think of this figure in terms of the low-level flow. The mass sink can be interpreted as a region of rising motion, where the air is

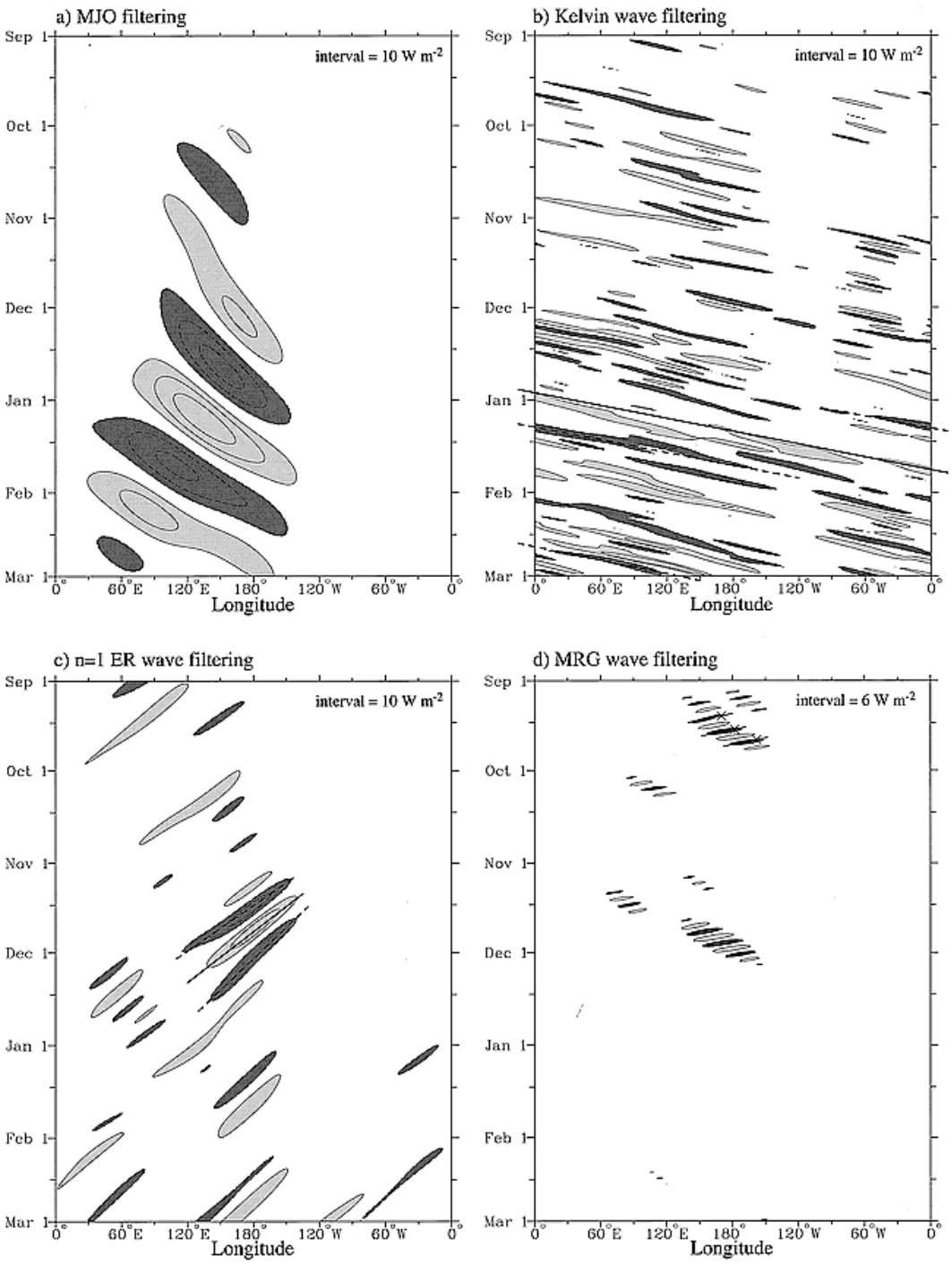

Figure 8: Longitudinal propagation of the Madden-Julian Oscillation (MJO; discussed later), Kelvin waves, equatorial Rossby (ER) waves, and mixed-Rossby-gravity (MRG) waves, as seen in the OLR. The zero contour has been omitted. The various modes are selected by including only the contributions from wave numbers and frequencies that fall in the corresponding boxes in Fig. 7. This is what is meant by "filtering." From Wheeler and Kiladis (1999).

Copyright David Randall, 2012

converging at low levels, e.g., in the western equatorial Pacific. The mass source can be interpreted as a region of sinking motion, where the air is diverging at low levels, e.g., in the eastern equatorial Pacific. (Unfortunately the mass sink is plotted on the east side and the mass source is plotted on the west side, but this does not really matter because the solution is periodic in the zonal direction anyway.) The model predicts strong westerlies converging (from the west, of course) at low levels into the region of rising motion, and low-level easterlies converging on the east side of the region of low-level convergence. The easterlies can be interpreted as the trades, and as the lower branch of the Walker circulation. The westerlies can be interpreted as a

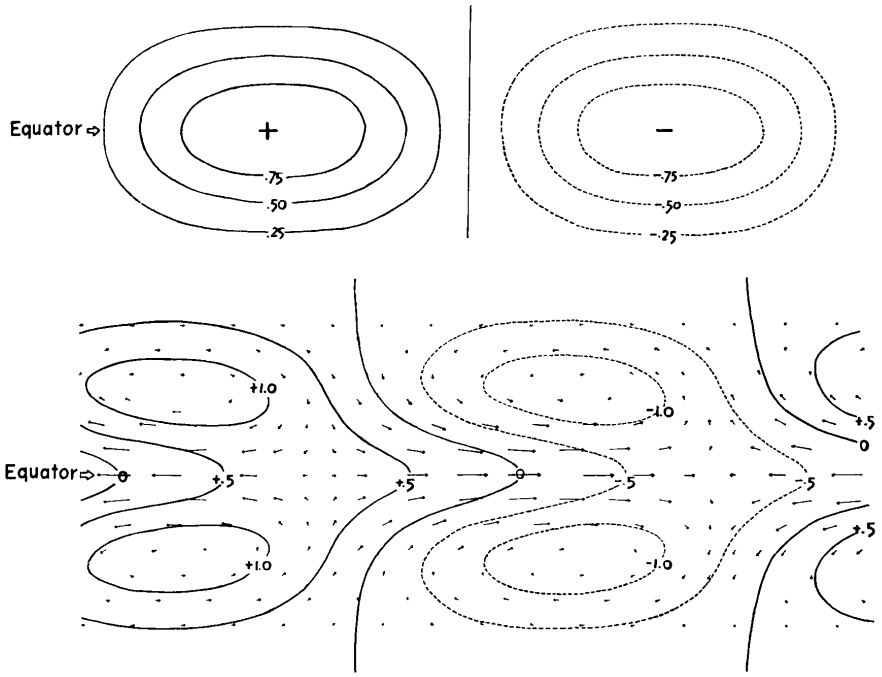

Figure 9: Stationary circulation pattern (lower panel) forced by the mass source and sink shown in the upper panel. From Matsuno (1966).

"monsoon-like" westerly inflow to a region of heating. Further discussion is given later.

Webster (1972) and Gill (1980) followed Matsuno's lead by developing simple analytic models of the response of a resting tropical atmosphere to heat sources and sinks. Since much of the convective heating in the tropics is confined over three relatively small land regions (Africa, South America, and the Indonesian region), Gill examined the atmospheric response to a relatively small-scale heating source that is centered on the equator. If the atmosphere is abruptly heated at some initial time, Kelvin waves propagate rapidly eastward and generate easterly trade winds to the east of the heating. Thus the easterly trade winds in the Pacific could result from Kelvin waves produced by convective heating over Indonesia. Similarly, Rossby waves propagate westward and generate westerlies to the west of the heating. Because the fastest Rossby wave travels at only one-third the speed of the Kelvin wave, the effects of the Rossby waves would be expected to reach only one-third as far those as those of the Kelvin wave. Gill

Copyright David Randall, 2012

interpreted the westerlies over the Indian ocean as a response to Rossby waves generated by convective heating over Indonesia.

Gill (1980; Fig. 10) studied what amounts to a steady-state version of Matsuno's model, and introduced forcing in the form of mass sources and sinks, along with very simple damping. In place of (2), we have

Figure 10: Adrian Gill, 1937-1986.

$$\varepsilon u - yv + \frac{\partial \phi}{\partial x} = 0 \,,$$

$$yu + \frac{\partial \phi}{\partial y} = 0 \,,$$

$$\varepsilon \phi + \frac{\partial u}{\partial x} + \frac{\partial v}{\partial y} = -Q \,, \tag{30}$$

and, as a purely diagnostic relation,

$$w = \varepsilon \phi + Q \,. \tag{31}$$

The wind components u and v represent the lower-tropospheric variables. In (30) and (31), ε^{-1} is a dissipation time scale, and Q is a "heating rate" that must be specified. The variables ϕ, w, and Q are defined in the middle troposphere. Gill included dissipation in the form of Rayleigh friction and Newtonian cooling, and for simplicity assumed that the time scales, given by ε^{-1}, are equal. Rayleigh friction is a simple parameterization of friction in which the velocity is divided by a frictional time scale. The friction term is neglected in the meridional momentum equation of (30); see Gill (1980) for an explanation.

Gill focused primarily on cases for which the heating is symmetric or anti-symmetric about the equator. As shown in Fig. 11, the solution for symmetric heating resembles a Walker circulation, with lower-tropospheric inflow into the heating region and upper-tropospheric outflow. The Walker Circulation is discussed in detail later in this Chapter. The surface easterlies cover a larger area than the surface westerlies because the phase speed of the eastward-propagating Kelvin wave is three times faster than that of the westward-moving Rossby wave. By forming a vorticity equation for the case of no damping, and then substituting from the continuity equation, Gill found that

$$v = yQ \,. \tag{32}$$

Copyright David Randall, 2012

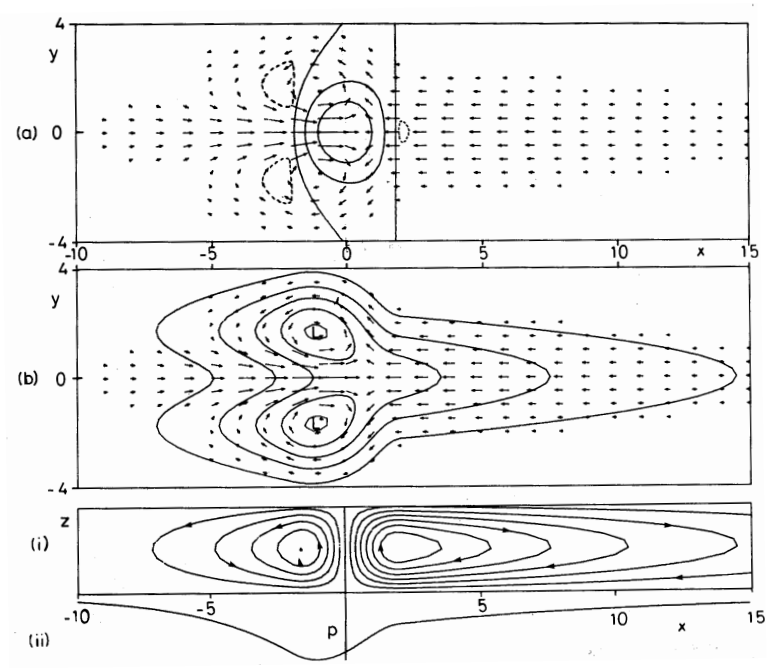

Figure 11: Solution of Gill's model for the case of heating symmetric about the Equator. The upper panel shows the heating field and the low-level wind field. The center panel shows the perturbation pressure field, which features low pressure along the Equator generally, with twin cyclones slightly off the Equator. The bottom panel shows the implied vertical motion and the zonal variation of the pressure along the Equator. From Gill (1980).

This is closely related to what is sometimes called "Sverdrup balance," in which the "meridional advection of the Coriolis parameter," i.e., the so-called β -term of the vorticity equation, is balanced by the divergence term, which is represented by the heating rate on the right-hand side of (32). For a incompressible atmosphere with a rigid lid at $z = D$ and a constant lapse rate, the gravest mode (the mode with the largest vertical scale) has horizontal velocity components that vary as $\cos(\pi z / D)$, i.e., they pass through zero in the middle troposphere. This is similar to the observed vertical structure of the Hadley-Walker circulation.

For $Q > 0$, (32) implies poleward motion in the lower layer and equatorward motion in the upper layer. This suggests that in regions of heating, e.g. the western Pacific, the Walker circulation produces a north-south circulation that opposes the Hadley circulation. Geisler (1981) found the same result. For $Q < 0$, the low-level motion is Equatorward; this is what we see in the subtropical highs, e.g., in the eastern Pacific.

The solution for anti-symmetric heating consists of a mixed Rossby-gravity wave and a Rossby wave. There is no Kelvin-wave response because the Kelvin wave is symmetric across the Equator. As a result, no response is generated to the east of the forcing region. Rossby and Yanai waves propagate slowly, and so are dissipated before they can propagate very far. As a result, the response to asymmetric heating is largely confined to the region slightly westward of the heating. To the west, the region of westerly flow into the heating region is limited because the Rossby modes travel slowly.

Copyright David Randall, 2012

Gill interpreted the symmetric case as a simulation of the Walker circulation, and the

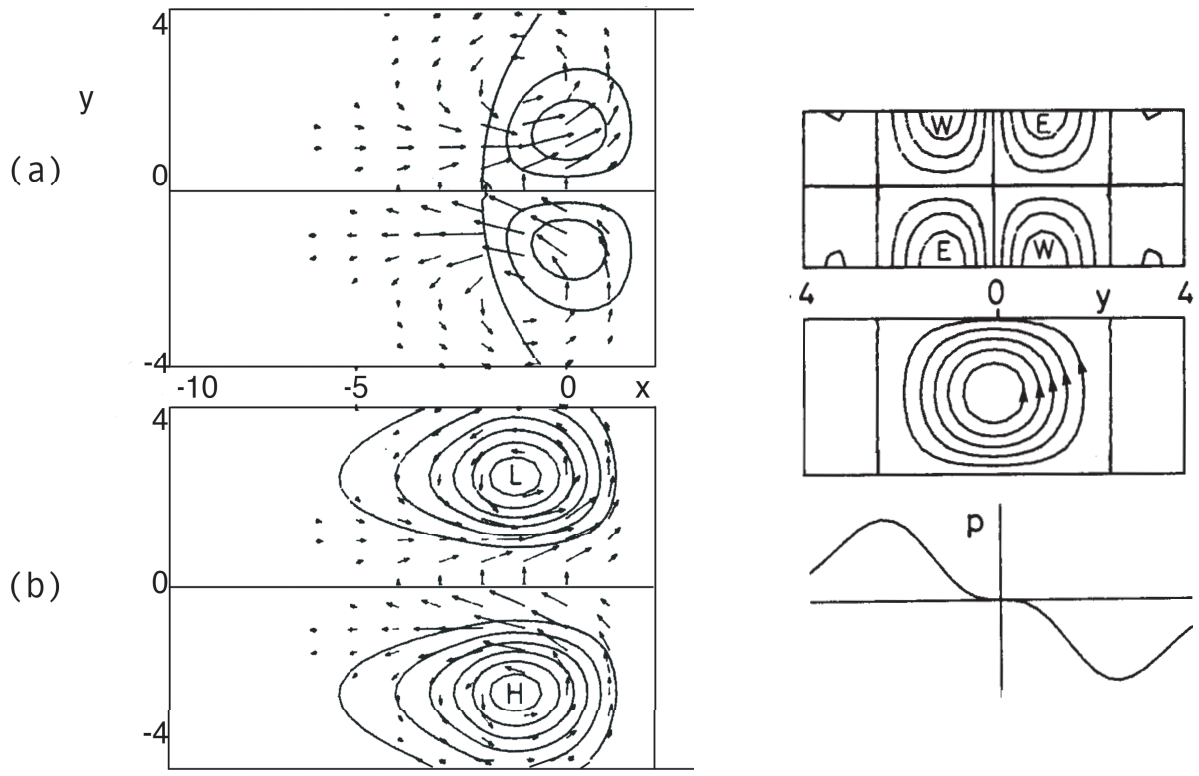

Figure 12: The response to antisymmetric heating. On the left side, the panel a) shows contours of the mid-level vertical velocity superimposed on the horizontal wind vectors for the lower layer. Panel b) shows contours of the perturbation surface pressure, again with the lower-layer horizontal wind field superimposed. The right-hand panels show the zonally integrated solution corresponding to the results in the left-hand panels. The upper right-hand panel shows the latitude-height distributions of the zonal velocity and the stream function of the mean meridional circulation, as well as the meridional profile of the surface pressure. From Gill (1980).

asymmetric case as a simulation of the Hadley circulation.

For heating centered on (symmetric about) the Equator, as in Fig. 11, Gill found strong westerlies on the west side, and strong easterlies on the east side, combining to give strong zonal convergence on the heating. The westerlies can be interpreted as the time-averaged response to westward -propagating Rossby waves excited by the heating, and the easterlies can be interpreted as the time-averaged response to eastward-propagating Kelvin waves excited by the heating. This implies a Walker circulation, as indicated in Fig. 11, and a surface pressure field with a minimum pressure slightly to the west of the heating.

When the heating is anti-symmetric across the Equator, as in Fig. 12, the model produces something like a Hadley circulation, with a low-level cyclonic circulation on the side with positive heating, and a low-level anticyclone on the other side.

Copyright David Randall, 2012

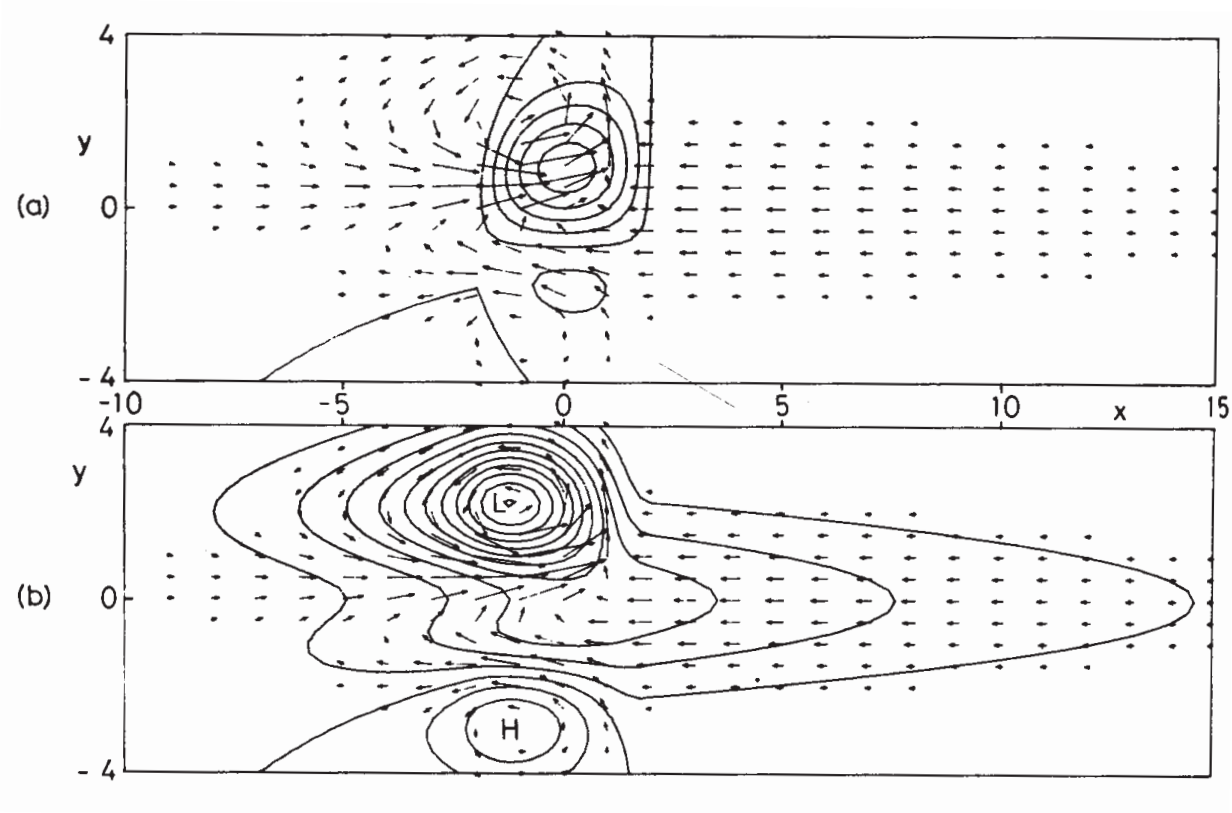

Figure 13: The response of Gill's model to a combination of symmetric and antisymmetric heating. From Gill (1980). Panel a) shows the heating, and panel b) shows the surface pressure. The low-level winds are shown in both panels.

When the symmetric and antisymmetric heatings are combined, as in Fig. 13, the model produces a circulation that looks remarkably similar to that of the Asian summer monsoon, as shown in Fig. 14.

Copyright David Randall, 2012

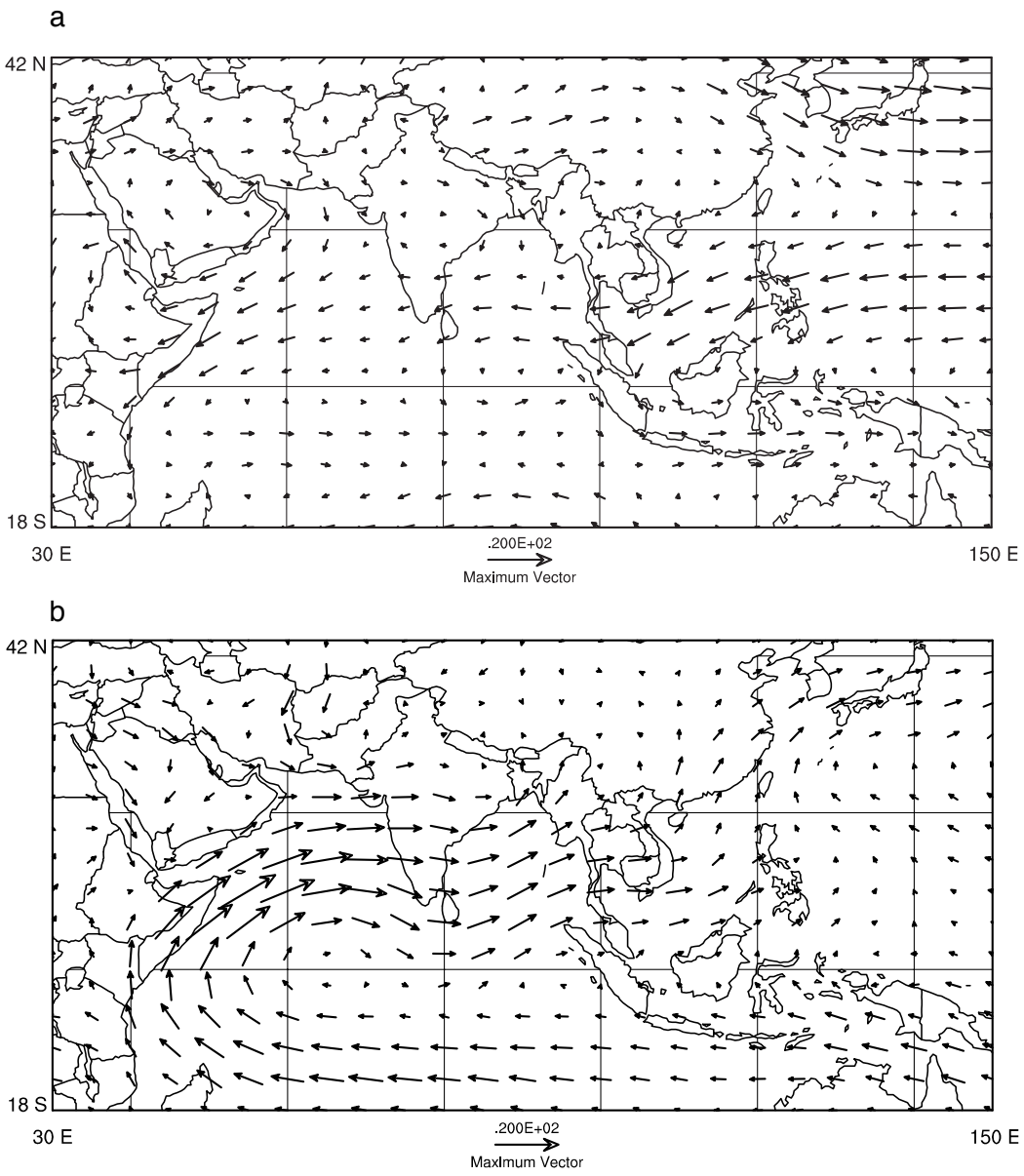

Figure 14: Observed 850 mb wind vectors for a) January, and b) July.

Copyright David Randall, 2012

References and Bibliography

Geisler, J. E., 1981: A linear model of the Walker circulation, *J. Atmos. Sci.*, **38**, 1390-1400.

Gill, A. E., 1980: Some simple solutions for heat-induced tropical circulation, *Q. J. Roy. Met. Soc.*, **106**, 447-462.

Gill, A. E., 1982: Studies of moisture effects in simple atmospheric models: The stable case. *Geophys. Astrophys. Fluid Dyn.*, **19**, 119-152.

Maruyama, T., and M. Yanai, 1967: Evidence of large-scale wave disturbances in the equatorial lower stratosphere. *J. Meteor. Soc. Japan*, **45**, 196-199.

Matsuno, T., 1966: Quasigeostrophic motions in the equatorial area. *J. Meteor. Soc. Japan*, **44**, 25-43.

Wallace, J. M., and V. E. Kousky, 1968: Observational evidence of Kelvin waves in the tropical stratosphere. *J. Atmos. Sci.*, **25**, 900-907.

Webster, P. J., 1972: Response of the tropical atmosphere to steady local forcing. *Mon. Wea. Rev.*, **100**, 518 - 541.

Wheeler, M. and G. N. Kiladis, 1999: Convectively coupled equatorial waves: analysis of clouds and temperature in the wavenumber-frequency domain. *J. Atmos. Sci.*, **56**, 374-399.

Yanai, M., and T. Maruyama, 1966: Stratospheric wave disturbances propagating over the equatorial Pacific. *J. Met. Soc. Japan*, **44**, 291-294.

Copyright David Randall, 2012